Measurement of Density and Shape for Single Black Carbon Aerosols in a Heavily Polluted Urban Area

Shurong Wang[a], Kaili Zhou[a], Xiaohui Lu[a], Hong Chen[a], Fan Yang[b], Qiang Li[c], Xin Yang[*a, d, e] and Xiaofei Wang[*a, d]

a. Shanghai Key Laboratory of Atmospheric Particle Pollution and Prevention, Department of Environmental Science and Engineering, Fudan University, Shanghai 200433, China
b. Environmental Monitoring Station of Pudong New District, Shanghai 200135, China
c. Cambustion Ltd., Cambridge CB1 8DH, United Kingdom
d. Shanghai Institute of Pollution Control and Ecological Security, Shanghai 200092, China
e. School of Environmental Science and Engineering, Southern University of Science and Technology, Shenzhen 518055, China

* Corresponding author:
Xiaofei Wang: Email: xiaofeiwang@fudan.edu.cn Tel: +86-21-31242526
Xin Yang: Email: yangxin@fudan.edu.cn Tel: +86-21-31245272

CONTENTS OF THIS FILE

Text S1-S3

Table S1

Figure S1

Text S1. The calibration for SP2 by Aquadag particle

A single-jet aerosol atomizer was used to produce Aquadag particles, which were then dried by a silica diffusion dryer and pass through the AAC-DMA system. For a group of Aquadag particles selected by AAC at a fixed $D_a$and DMA at a fixed D_m,the Aquadag particles' mass (m_p) can be derived by Eq. (1)-(3):

$$B = \frac{C_c(D_m)}{3\pi\mu D_m} \quad (1)$$

$$\tau = \frac{\rho_0 C_c(D_a) {D_a}^2}{18\mu} \quad (2)$$

$$m_p = \frac{\tau}{B} \quad (3)$$

Then the SP2 was utilized to measure the mass of these AAC-DMA selected Aquadag particles, producing a mass frequency distribution, whose peak location served as m_{BC}. Theoretically, m_{BC} should be equal to m_p for Aquadag particle, while there is a difference (~±5%) between these two values due to the uncertainties of the measurement of D_a, D_m and m_{BC} by using AAC, DMA and SP2. Given that the operating parameters of AAC, DMA and SP2 were consistent between the calibration and sampling process, thus the precision for m_{BC} of particles selected by AAC and DMA was found to be ~±5% during this study. Besides, SP2 was more sensitive to Aquadag aerosol than to other BC types (e.g., fullerene and diesel exhaust), since the Aquadag induces a higher incandescence signal peak (by a factor of ~25 %) than ambient BC with the same mass (Laborde et al., 2012; Wu et al., 2019). Therefore, like many previous studies (Laborde et al., 2013; Liu et al., 2019a; Liu et al., 2019b; Zhao et al., 2019), during the calibration process the broadband incandescent signal was corrected by scaling a factor of 0.75 to avoid overestimation resulting from the Aquadag-based calibration curve. Table S2 shows several groups of calibration data of SP2 by using this method.

Text S2. Uncertainty estimation for the measured and derived parameters.

1. The uncertainty for the aerodynamic diameter (D_a).

For balanced flows (when the exhaust flow equals the sheath flow) the relaxation time at the center of the transfer function of the AAC, can be calculated by Eq. (1).

$$\tau = \frac{2Q_{sh}}{4\pi\omega^2 r^2 L} \quad (1)$$

Thus, the uncertainty of ε_τ/τ can be calculated as ~ 10% in Eq. (2), where $\varepsilon_{Q_{sh}}$ =0.1 L/ min, ε_ω=5 rpm, ε_L=2 mm and $\varepsilon_{\bar{r}}$=5 μm (Tavakoli and Olfert, 2014).

$$(\frac{\varepsilon_\tau}{\tau})^2 = (\frac{\varepsilon_{Q_{sh}}}{Q_{sh}})^2 + 4(\frac{\varepsilon_\omega}{\omega})^2 + 4(\frac{\varepsilon_{\bar{r}}}{\bar{r}})^2 + (\frac{\varepsilon_L}{L})^2 \quad (2)$$

Meanwhile, the relationship of D_a and τ can be expressed as:

$$\tau = \frac{\rho_0 C_c(D_a) {D_a}^2}{18\mu} \quad (3)$$

therefore, the uncertainty for the D_a was found to be 8% according to Eq. (4), where ε_μ is calculated using a temperature uncertainty of 4 °C, resulting in ε_μ/μ= 1.2%. It is assumed that the uncertainty of slip corrections, ε_{C_c}/C_c, is the same for all particle sizes and equals 2.1% (Allen and Raabe, 1985)

$$(\frac{\varepsilon_{D_a}}{D_a})^2 = \sqrt{0.5}(\frac{\varepsilon_\tau}{\tau})^2 + \sqrt{0.5}(\frac{\varepsilon_\mu}{\mu})^2 + \sqrt{0.5}(\frac{\varepsilon_{C_c}}{C_c})^2 \quad (4)$$

(1) The uncertainty for the particle mass (m_p).

According to the definition of the particle relaxation time in Eq. (5), where B is the mobility of particle.

$$\tau = Bm_p \quad (5)$$

$$B = \frac{C_c(D_m)}{3\pi\mu D_m} \quad (6)$$

The uncertainty for B can be derived by Eq. (7), where ε_{D_m} $/D_m$= 3%(Kinney et al., 1991)

$$(\frac{\varepsilon_B}{B})^2 = (\frac{\varepsilon_{D_m}}{D_m})^2 + (\frac{\varepsilon_\mu}{\mu})^2 + (\frac{\varepsilon_{C_c}}{C_c})^2 \quad (7)$$

Therefore, the uncertainty for particle mass was found to be ~11% via Eq. (8).

$$(\frac{\varepsilon_{m_p}}{m_p})^2 = (\frac{\varepsilon_\tau}{\tau})^2 + (\frac{\varepsilon_B}{B})^2 \quad (8)$$

2. The uncertainty for the effective density of particle.

The effective density is defined in Eq. (9), thus, the uncertainty in effective density is

14% according to Eq. (10).

$$\rho_{eff} = \frac{m_p}{\frac{\pi}{6}{D_m}^3} \quad (9)$$

$$(\frac{\varepsilon_{\rho_{eff}}}{\rho_{eff}})^2 = 9(\frac{\varepsilon_{D_m}}{D_m})^2 + (\frac{\varepsilon_{m_p}}{m_p})^2 \quad (10)$$

3. The uncertainty of the dynamic shape factor (χ).

Given that the relationship between the aerodynamic diameter and volume equivalent diameter is (DeCarlo et al., 2004):

$$D_a = D_{ve}\sqrt{\frac{1\rho_p C_c(D_{ve})}{\chi\, \rho_0 C_c(D_a)}} \quad (11)$$

The relationship between the D_m and D_{ve} is:

$$\chi = \frac{C_c(D_{ve})D_m}{C_c(D_m)D_{ve}} \quad (12)$$

Therefore, the dynamic shape factor can be expressed as:

$$\chi = (\frac{D_m}{D_a C_c(D_m)})^{2/3} \frac{{\rho_p}^{1/3} C_c(D_{ve})}{{\rho_0}^{1/3} {C_c}^{1/3}(D_a)} \quad (13)$$

Here, like the previous study (Moteki et al., 2010), the accuracy of the BC-dominated particle density (1.8 g cm^{-3}) were adopted 5% based on a range of reported values (Mullins and Williams, 1987; Park et al., 2004), namely, $\varepsilon_{\rho_p}/\rho_p$= 5%. The uncertainty for the χ can be calculated as 9% via Eq. (14), where ($\varepsilon_{C_c(D_{ve})}/C_c(D_{ve})$)= ($\varepsilon_{C_c(D_a)}/C_c(D_a)$)= ($\varepsilon_{C_c(D_m)}/C_c(D_m)$)=2.1 % (Allen and Raabe, 1985).

$$(\frac{\varepsilon_\chi}{\chi})^2 = \frac{4}{9}(\frac{\varepsilon_{D_m}}{D_m})^2 + \frac{4}{9}(\frac{\varepsilon_{D_a}}{D_a})^2 + \frac{14}{9}(\frac{\varepsilon_{C_c}}{C_c})^2 + \frac{1}{9}(\frac{\varepsilon_{\rho_p}}{\rho_p})^2 \quad (14)$$

Text S3. Calculation of the number of 3 types of particle: Non-BC particle, BC-dominated particle and BC-mixed particle.

The number of Non-BC particle ($N_{non\text{-}BC}$) and BC-containing particle ($N_{BC\text{-}containing}$) can be obtained by SP2. BC-containing particle includes BC-dominated particle and BC-mixed particle. The number of BC-dominated particle ($N_{BC\text{-}dominated}$) were calculated through module method (Gauss fitting in IGOR Pro software), X axis is the mass of BC (M_{BC}) in single particle, Y axis is the dN/dM_{BC} (N means "particle number"), thus $N_{BC\text{-}dominated}$ is exactly the area of the fitted peak. Finally, the number of BC-mixed particle ($N_{BC\text{-}mixed}$) was known according to the relationship, "$N_{BC\text{-}mixed} = N_{BC\text{-}containing} - N_{BC\text{-}dominated}$"

Table S1. The sampling periods for particles with three different aerodynamic diameters (200nm, 350nm and 500nm) are respectively showed in (a), (b) and (c).

(a)

	AAC-SMPS			AAC-DMA-SP2
D_a=200nm	24 Nov 2018 18:30-20:30 25 Nov 2018 10:30-12:30 26 Nov 2018 8:30-10:30 27 Nov 2018 14:30-16:30 28 Nov 2018 12:30-14:30 29 Nov 2018 16:30-18:30	15 Aug 2019 18:00- 16 Aug 2019 18:00	D_a=200nm, D_m=135nm	9 Sept 2019 00:00-24:00 10 Sept 2019 00:00-24:00 11 Sept 2019 00:00-24:00 12 Sept 2019 00:00-24:00 13 Sept 2019 00:00-24:00 14 Sept 2019 00:00-24:00

(b)

	AAC-SMPS		AAC-DMA-SP2
D_a=350nm	27 Aug 2019 22:00-23:00 28 Aug 2019 12:00-13:00 29 Aug 2019 17:00-18:00 30 Aug 2019 16:30-17:30 31 Aug 2019 19:30-20:30	D_a=350nm, D_m=260nm	27 Aug 2019 22:00-28 Aug 2019 22:00 28 Aug 2019 22:00-29 Aug 2019 22:00 29 Aug 2019 22:00-30 Aug 2019 22:00 30 Aug 2019 22:00-31 Aug 2019 22:00 31 Aug 2019 22:00-1 Sept 2019 22:00

(c)

	AAC-SMPS		AAC-DMA-SP2
D_a=500nm	22 Aug 2019 20:00-22:00 23 Aug 2019 14:00-16:00 24 Aug 2019 8:00-10:00 25 Aug 2019 22:00-24:00 26 Aug 2019 20:00-22:00	D_a=500nm, D_m=359nm	22 Aug 2019 22:00-23 Aug 2019 22:00 23 Aug 2019 22:00-24 Aug 2019 22:00 24 Aug 2019 22:00-25 Aug 2019 22:00 25 Aug 2019 22:00-26 Aug 2019 22:00 26 Aug 2019 22:00-27 Aug 2019 22:00

Table S2. Calibration data of SP2 by using AAC-DMA tandem system to quantify the mass of BC standard particle.

Group	D_a(nm)	D_m(nm)	m_{BC}(fg)	D_{ve}(nm)	Shape Factor (χ)
1	70	91	0.29	67	1.7
2	100	118	0.69	90	1.6
3	120	141	1.18	108	1.6
4	140	175	2.05	130	1.6
5	160	202	3.07	148	1.6
6	200	241	5.53	180	1.5
7	250	300	10.57	224	1.5
8	350	445	30.71	319	1.5
9	450	496	53.92	385	1.4
10	500	594	80.81	441	1.4

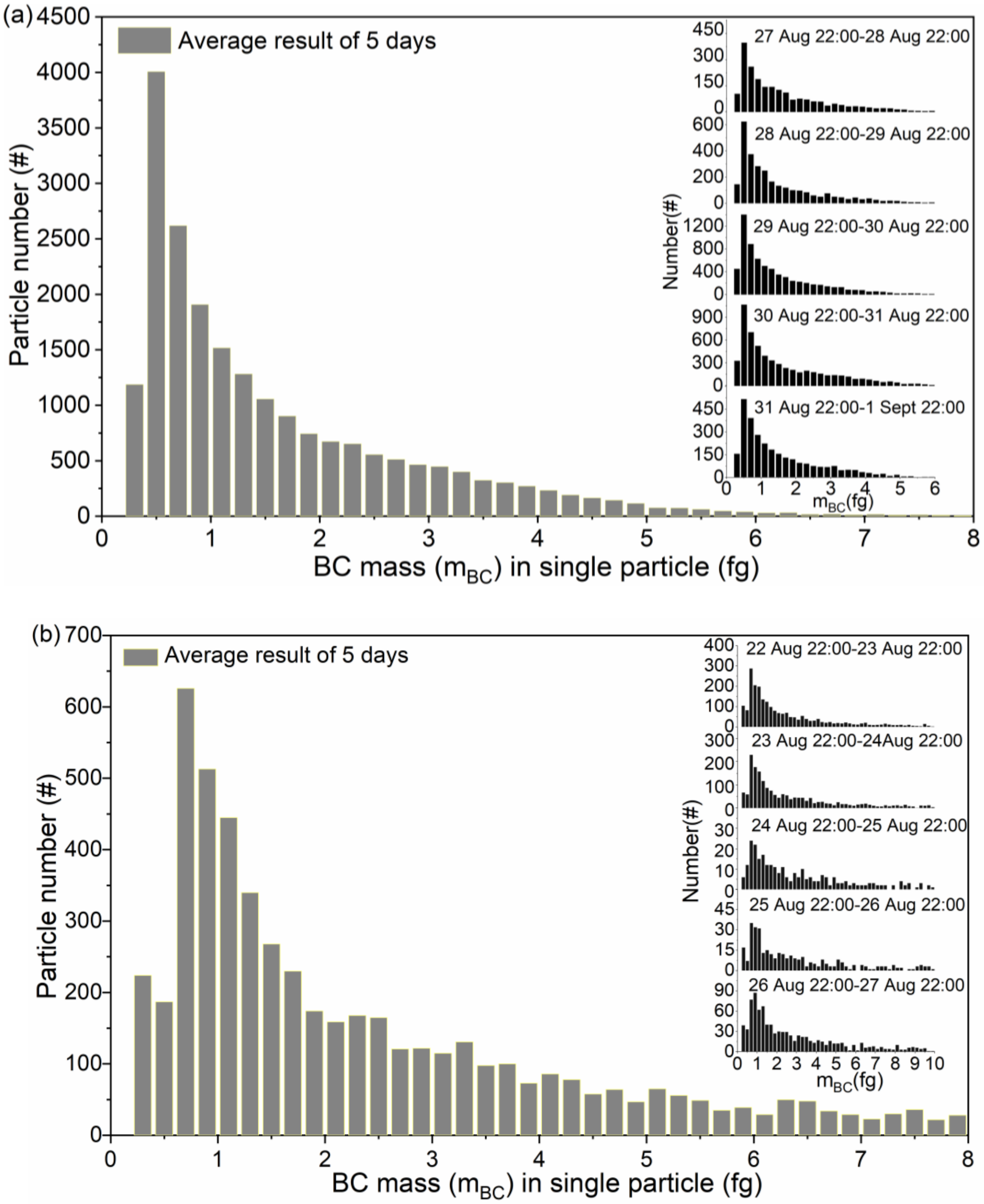

Figure S1. BC mass distribution of single particle in **(a)** Mode (D_a =350 nm,D_m =260 nm) and **(b)** Mode (D_a =500 nm, D_m =359nm), the insert panel shows the daily average BC mass distribution.

Reference

Allen, M.D., Raabe, O.G. (1985). Slip Correction Measurements of Spherical Solid Aerosol Particles in an Improved Millikan Apparatus. Aerosol Science and Technology 4, 269-286. https://doi.org/10.1080/02786828508959055

DeCarlo, P.F., Slowik, J.G., Worsnop, D.R., Davidovits, P., Jimenez, J.L. (2004). Particle morphology and density characterization by combined mobility and aerodynamic diameter measurements. Part 1: Theory. Aerosol Science and Technology 38, 1185-1205. https://doi.org/10.1080/027868290903907

Kinney, P.D., Pui, D.Y.H., Mulholland, G.W., Bryner, N.P. (1991). USE OF THE ELECTROSTATIC CLASSIFICATION METHOD TO SIZE 0.1 MU-M SRM PARTICLES - A FEASIBILITY STUDY. Journal of Research of the National Institute of Standards and Technology 96, 147-176. https://doi.org/10.6028/jres.096.006

Laborde, M., Crippa, M., Tritscher, T., Jurányi, Z., DeCarlo, P., Temime-Roussel, B., Marchand, N., Eckhardt, S., Stohl, A., Baltensperger, U., Prevot, A., Weingartner, E., Gysel, M. (2013). Black carbon physical properties and mixing state in the European megacity Paris. Atmos. Chem. Phys. 13, 5831-5856. https://doi.org/10.5194/acp-13-5831-2013

Laborde, M., Mertes, P., Zieger, P., Dommen, J., Baltensperger, U., Gysel, M. (2012). Sensitivity of the Single Particle Soot Photometer to different black carbon types. Atmospheric Measurement Techniques 5, 1031-1043. https://doi.org/10.5194/amt-5-1031-2012

Liu, D., Joshi, R., Wang, J., Yu, C., Allan, J.D., Coe, H., Flynn, M.J., Xie, C., Lee, J., Squires, F., Kotthaus, S., Grimmond, S., Ge, X., Sun, Y., Fu, P. (2019a). Contrasting physical properties of black carbon in urban Beijing between winter and summer. Atmos. Chem. Phys. 19, 6749-6769. https://doi.org/10.5194/acp-19-6749-2019

Liu, H., Pan, X., Wu, Y., Wang, D., Tian, Y., Liu, X., Lei, L., Sun, Y., Fu, P., Wang, Z. (2019b). Effective densities of soot particles and their relationships with the mixing state at an urban site of the Beijing mega-city in the winter of 2018. Atmospheric Chemistry and Physics Discussions, 1-25. https://doi.org/10.5194/acp-2019-526

Moteki, N., Kondo, Y., Nakamura, S.-i. (2010). Method to measure refractive indices of small nonspherical particles: Application to black carbon particles. Journal of Aerosol Science 41, 513-521. https://doi.org/10.1016/j.jaerosci.2010.02.013

Mullins, J., Williams, A. (1987). The optical properties of soot: a comparison between experimental and theoretical values. Fuel 66, 277-280. https://doi.org/https://doi.org/10.1016/0016-2361(87)90255-9

Park, K., Kittelson, D.B., Zachariah, M.R., McMurry, P.H. (2004). Measurement of Inherent Material Density of Nanoparticle Agglomerates. Journal of Nanoparticle Research 6, 267-272. https://doi.org/http://dx.doi.org/10.1023/B:NANO.0000034657.71309.e6

Tavakoli, F., Olfert, J.S. (2014). Determination of particle mass, effective density, mass–mobility exponent, and dynamic shape factor using an aerodynamic aerosol

classifier and a differential mobility analyzer in tandem. Journal of Aerosol Science 75, 35-42. https://doi.org/https://doi.org/10.1016/j.jaerosci.2014.04.010
Wu, Y., Xia, Y., Huang, R., Deng, Z., Tian, P., Xia, X., Zhang, R. (2019). A study of the morphology and effective density of externally mixed black carbon aerosols in ambient air using a size-resolved single-particle soot photometer (SP2). Atmos. Meas. Tech. 12, 4347-4359. https://doi.org/10.5194/amt-12-4347-2019
Zhao, D., Huang, M., Tian, P., He, H., Lowe, D., Zhou, W., Sheng, J., Wang, F., Bi, K., Kong, S., Yang, Y., Liu, Q., Liu, D., Ding, D. (2019). Vertical characteristics of black carbon physical properties over Beijing region in warm and cold seasons. Atmospheric Environment 213, 296-310. https://doi.org/https://doi.org/10.1016/j.atmosenv.2019.06.007